

# The Visibility-Spectrum Relation among Radio Loud AGNs

Seiji KAMENO<sup>1,2</sup>, Makoto INOUE<sup>2</sup>, Kin'ya MATSUMOTO<sup>2,3</sup>, Hiroshi TAKABA<sup>4</sup>,  
Takahiro IWATA<sup>4</sup>, Rendong NAN<sup>5</sup>, and Richard T. SCHILIZZI<sup>6</sup>

<sup>1</sup>*The University of Tokyo, Bunkyo, Tokyo 113, Japan*

<sup>2</sup>*Nobeyama Radio Observatory/NAO, Minamimaki, Nagano 384-13, Japan*

<sup>3</sup>*The University of Electro-Communications, Chofu, Tokyo 182, Japan*

<sup>4</sup>*Kashima Space Research Center/CRL, Kashima, Ibaraki 314, Japan*

<sup>5</sup>*Beijing Astronomical Observatory, Beijing, China*

<sup>6</sup>*Radiosterrewacht Dwingeloo, Dwingeloo, The Netherlands*

**Abstract.** We report the results from the first millimeter-VLBI radio source survey using Kashima-Nobeyama baseline Interferometer (KNIFE). We have already observed 69 flat-spectrum sources (FSS) and 18 compact steep-spectrum (CSS) sources, and detected 50 and 9, respectively. A correlation between visibility at 22 GHz and spectral index in millimeter wavelength indicates that a simple two-component model consisting of flat-spectrum core and steep-spectrum lobes is acceptable among radio-loud active galactic nuclei (AGN) in general.

## 1. Introduction

A survey for extragalactic radio sources allows us to investigate the nature of active galactic nuclei (AGN). VLBI observations function as a spatial filter to pick up compact components like cores, while single dish observations are smeared by extended components like jets and radio lobes. Hence, a VLBI survey is a powerful tool for statistical study of the activities of AGN cores. Comparing total and correlated flux density, we can measure the emissions from both compact and extended components.

As widely known, AGNs are classified into two groups; radio-loud and radio-quiet objects. Even though both classes have almost the same spectral energy distribution (SED) from far-infrared to ultraviolet wavelengths, the radio-to-optical luminosity ratio of the radio-loud AGN is  $10^3 \sim 10^5$  times as large as one of the radio-quiet (SANDERS *et al.*, 1989). Core flux density derived from VLBI survey will play an important role to measure the correct SED, which reflects current activity.

PRESTON *et al.*, (1985) made a systematic VLBI full-sky survey at 2.29 GHz using deep space network (DSN) antennas. They observed 1398 sources and detected 917 with fringe spacings of  $\sim 3$  milliarcsec (mas). They also made 8.4-GHz survey for 416 sources and detected 278 at  $\sim 1$  mas fringe spacings (MORABITO *et al.*, 1986).

PEARSON and READHEAD (1988) conducted VLBI survey at 5 GHz for 65 sources and made images with a resolution of  $\sim 1$  mas for 37 sources. Such images enabled structural classification and study about relations between structural class and other properties such as spectral index, polarization, and variability.

Unlike low-frequency VLBI observations, millimeter or near-millimeter VLBI observations are very efficient in detecting the core component, since the high-frequency observations are much less affected by the complex jet structure and/or synchrotron self-absorption. VALTAOJA *et al.*, (1992) compiled 22, 37, 90, and 230 GHz single-dish and 2.3, 8.4, and 22 GHz VLBI data. 19 samples detected by 22-GHz VLBI are included in their list.

We report the results from the first millimeter-VLBI survey using Kashima-Nobeyama baseline VLBI (KNIFE) at 22 and 43 GHz for 69 FSSs (MATSUMOTO *et al.*, 1994). KNIFE consists of the CRL Kashima 34-m and the NRO Nobeyama 45-m radio telescopes with a 197-km east-west baseline, and provides fringe spacings of 7 and 14 mas at 22 and 43 GHz, respectively. In addition to FSSs, 18 CSSs also have been observed (KAMENO *et al.*, in preparation). The relation of the visibility and spectrum will be discussed in this paper.

## 2. The Samples and Observations

The 69 FSS samples from KNIFE survey (MATSUMOTO *et al.*, 1994) and 18 CSS samples (KAMENO *et al.*, in preparation) are included in our samples. The FSSs are selected from the list of PRESTON *et al.*, (1985), MORABITO *et al.*, (1986), and ABRAHAM *et al.*, (1984). The CSS are derived from FANTI *et al.*, (1990) and 18 samples whose extrapolated flux density at 22 GHz is more than 0.5 Jy are selected.

Observational status is listed in Tables 1 and 2. Correlation processing was conducted by Kashima K-3 correlator and NAOCO (see SHIBATA *et al.*, in these Proceedings) for FSS and CSS observations, respectively. The correlated data were integrated coherently for 64 seconds and averaged over 16 frequency channels. Correlated flux density is derived using the relation,

$$S_c = \frac{2k\sqrt{T_{s1}T_{s2}}}{A_{e1}A_{e2}} L_c^{-1} \rho,$$

Table 1. KNIFE survey for FSSs and CSSs.

Date	Target	Frequency	Remarks
6/10/90	FSS	22.2 GHz	VLBI
11/4/90	FSS	22.2 GHz	VLBI
11/9/90	FSS	43.1 GHz	VLBI
23/4/92	CSS	42.8 GHz	VLBI, single dish
24/4/92	CSS	22.2 GHz	VLBI, single dish
25/4/92	CSS	92.0 GHz	single dish

Table 2. The performance of the KNIFE.

Frequency	22 GHz		43 GHz	
Station	NRO	CRL	NRO	CRL
Aperture efficiency	0.65	0.63	0.50	0.45
$T_{\text{sys}}$	150 K	170 K	150 K	1500 K
Bandwidth	2 MHz $\times$ 16 CH			
Terminal	K-4 type 0			
Baseline	197 km east-west			
Sensitivity	0.122 %/Jy		0.023 %/Jy	
Fringe spacing	14 mas		7 mas	

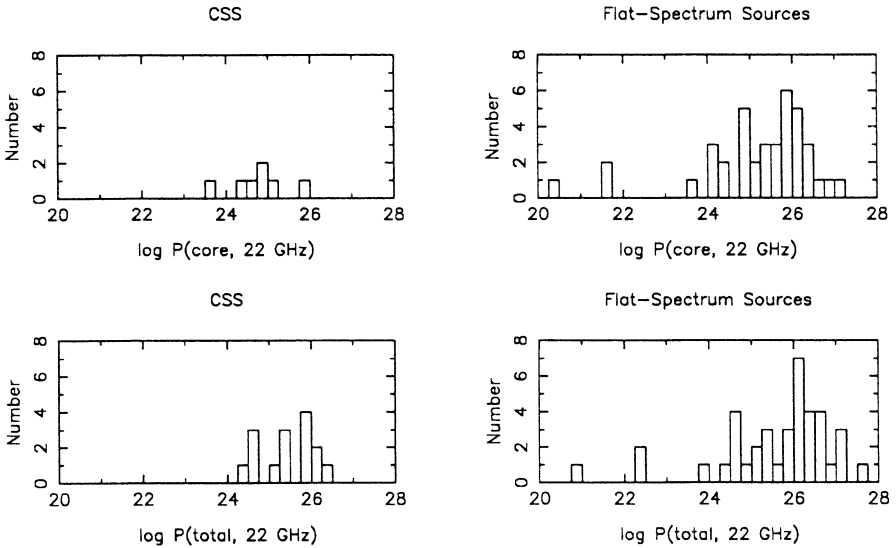


Fig. 1. The histogram of the monochromatic luminosity of our samples at 22 GHz. We assumed the Hubble constant  $H_0 = 100 \text{ km sec}^{-1} \text{ Mpc}^{-1}$  and the deceleration parameter  $q_0 = 0.5$ . Top left: Core component of CSS. The median is  $9.1 \times 10^{24} \text{ W/Hz}$ . Top right: Core component of FSS. The median is  $4.7 \times 10^{25} \text{ W/Hz}$ . Bottom left: Total component of CSS. The median is  $6.0 \times 10^{25} \text{ W/Hz}$ . Bottom right: Total component of FSS. The median is  $1.0 \times 10^{26} \text{ W/Hz}$ .

where  $S_c$  is correlated flux density,  $k$  the Boltzman constant,  $T_s$  system noise temperature,  $A_e$  effective area of antenna aperture,  $L_c$  coherence loss factor and  $\rho$  normalized correlation coefficient. System noise temperature was measured for each scan at each station. Coherence loss factor was derived from the observation of strong sources for each session. Typical error of the correlated flux is  $\sim 10\%$  and the detection limit of  $7\sigma$  is 0.2 and 0.5 Jy at 22 and 43 GHz, respectively.

The number of detected sources is 50 and 20 FSSs and 9 and 3 CSSs at 22 and

43 GHz, respectively. The total and correlated luminosity ranges of our sample are shown in Fig. 1.

### 3. Results and Discussions

Figure 2 shows the visibility-spectrum relation of CSSs. For detected nine samples, a strong correlation can be seen. The correlation coefficient is 0.81 and the confidence level is more than 90%. Adding 50 flat-spectrum sources in Fig. 3, identical relation can be seen.

This relation is acceptable for the standard model of radio sources; a compact core shows flat-spectrum and extended jets and lobes show steep-spectrum. If the core component dominates in total flux density, the visibility will be large up to 1 and the spectrum will be flat (e.g. 2145 + 06). If the lobe component is dominant, the visibility will be small and the spectrum will be steep (e.g. 3C286)

A two-component model consisting of compact flat-spectrum component (core) and extended steep-spectrum component (lobe) is simple and useful to understand this relation. We tried model fitting using this two-component model. Our assumptions are: 1. core is so compact that even VLBI observations cannot resolve it out, 2. lobe is wide enough to be resolved out completely, 3. core component is optically thick in wavelength longer than a centimeter, and 4. core component is optically thin in millimeter wavelength and has flat-spectrum ( $\alpha_{\text{core}} = -0.15$ ). The free parameters are the turnover frequency of the core ( $\nu_{\text{max}}$ ), the spectrum index of the lobe at 22 GHz ( $\alpha_{\text{lobe}}$ ). The solid line in Fig. 3 indicates

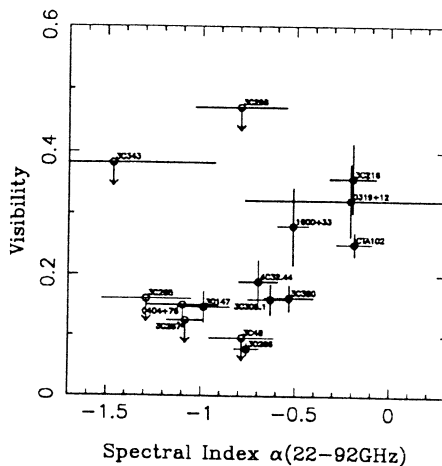


Fig. 2. Spectral index versus visibility of CSS at 22 GHz. There is a strong positive correlation between spectral index and core dominance. The correlation coefficient is 0.81, whose confidence level is greater than 95%.

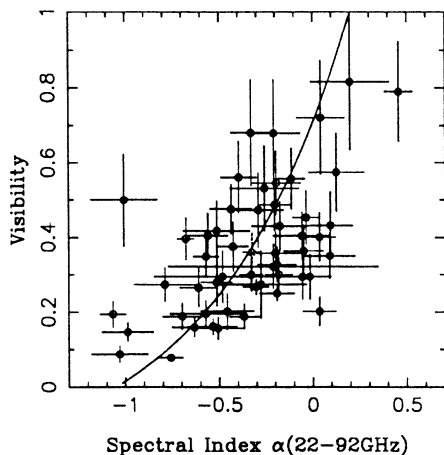


Fig. 3. Spectral index in mm-waves (*horizontal*) versus visibility (*vertical*). Eight CSSs (*filled circle*) and 50 active sources observed with KNIFE (*open circle*) are plotted. The solid line indicates the two-component model at  $v_{\max} = 56$  GHz and  $\alpha_{\text{lobe}} = -1.05$ .

$v_{\max} = 56$  GHz and  $\alpha_{\text{lobe}} = -1.05$ . More than 90% sources are included in range of  $v_{\max} = 56 \pm 17$  GHz and  $\alpha_{\text{lobe}} = -1.05^{+0.4}_{-0.7}$ .

Our results indicate that the spectral property of the core and the lobes are almost the same in every source. The core-to-lobe flux density ratio is a significant parameter to shape the total integrated spectra.

CSSs are located in small-visibility and steep-spectrum region in Fig. 2. However the core component of all three sources detected in 43-GHz VLBI (1600 + 335, 3C380, and CTA102) showed flat-spectrum between 22 and 43 GHz ( $-0.1 < \alpha_{\text{core}} < 0.7$ ). Comparing the millimeter and centimeter VLBI flux density, other CSSs also indicate that the flat-spectrum core component exists. Thus the difference between CSS and flat-spectrum sources should be confined in the structure of the lobes.

We tested whether the Doppler boosting effect result in the variety of the core-to-lobe flux density ratio. If beaming is effective for the amplification of the core component and spectral flattening, superluminal radio sources will be located in large-visibility and flat-spectrum region in Fig. 2. However, no significant differences are seen between superluminal and non-superluminal sources (see Fig. 4).

The optical-to-radio luminosity ratio  $r (= \log[vF_{\nu}(\text{optical})/vF_{\nu}(\text{radio})])$  is shown in Fig. 5. The range in our radio-loud sample is  $0.4 < r < 2.3$  and the median is  $r = 1.3$ , while  $r = 4\sim 5$  for radio-quiet quasars (SANDERS *et al.*, 1989). We conclude that the difference of the  $r$  between radio-loud and radio-quiet objects is of core origin, not the result of the emission from the jets and the lobes. More detailed observations in radio-emitting mechanism in the core are necessary to unify these two classes of AGN.

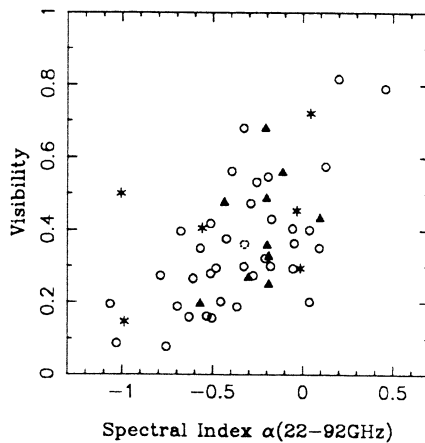


Fig. 4. Superluminal motion and the visibility-spectrum diagram. Superluminal radio sources (*filled triangle*), subluminal sources (*asterisk*), and non-superluminal sources (*open circle*) are plotted. No significant relation can be seen.

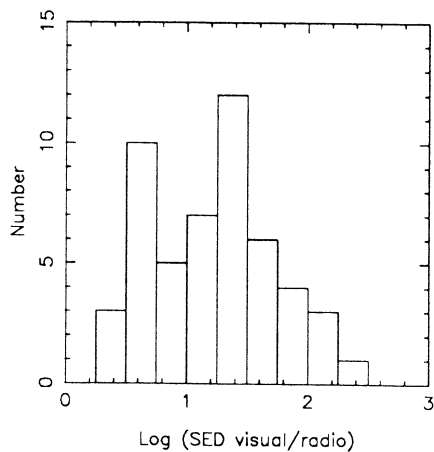


Fig. 5. Histogram of the optical-to-radio luminosity ratio  $r = \log[vF_{\nu}(\text{optical})/vF_{\nu}(\text{radio})]$ . Correlated flux density at 22 GHz was adopted for  $F_{\nu}(\text{radio})$ . The median value is 1.3.

#### 4. Conclusion

A sensitive 22- and 43-GHz VLBI survey using KNIFE is going on. Such a high-frequency VLBI survey allows statistical study for activities of the core in

AGN. Using detected 59 samples, we found the visibility-spectrum relation. A simple two-component model consists of flat-spectrum core and steep-spectrum lobe suitably explains the relation. Most of our sample have the turnover frequency of core component in millimeter-wavelength. CSSs also follow this model.

We found no relationship between visibility-spectrum diagram and superluminal motion.

Comparing radio-to-optical luminosity ratio of VLBI core component in radio-loud AGNs to radio-quiet one, we conclude that the difference between two classes originates in the core.

#### REFERENCES

- ABRAHAM, Z., MEDEIROS, J. R. and KAUFMANN, P. (1984): *Astron. J.*, **89**, 200.
- FANTI, R., FANTI, C., SCHILIZZI, R. T., SPENCER, R. E., NAN, R., PARMA, P., VAN BREUGEL, W. J. M. and VENTURI, T. (1990): *Astron. Astrophys.*, **231**, 333.
- KAMENO, S., INOUE, M., MATSUMOTO, M., TAKABA, H., IWATA, T., TAKAHASHI, Y., KOYAMA, Y., NAN, R. and SCHILIZZI, R. T., in preparation.
- MATSUMOTO, K., TAKABA, H., IWATA, T., KURIHARA, N., KAWAGUCHI, N., INOUE, M., MIYOSHI, M. and KAMENO, S. (1994): submitted to *J. Geod. Soc. Japan*.
- MORABITO, D. D., NIELL, A. E., PRESTON, R. A., LINFIELD, R. P., WEHRLE, A. E. and FAULKNER, J. (1986): *Astron. J.*, **91**, 1038 .
- PEARSON, T. J. and READHEAD, A. C. S. (1988): *Astrophys. J.*, **328**, 114.
- PRESTON, R. A., MORABITO, D. D., WILLIAMS, J. G., FAULKNER, J., JAUNCEY, D. L. and NICOLSON, G. D. (1985): *Astron. J.*, **90**, 1599.
- SANDERS, D. B., PHINNEY, E. S., NEUGEBAUER, G., SOIFER, B. T. and MATTHEWS, K. (1989): *Astrophys. J.*, **347**, 29.
- SHIBATA, K., SASAO, T., KAWAGUCHI, N., TAMURA, Y., KAMENO, S., MIYOSHI, M., ASARI, K., MANABE, S., HARA, T., KUJI, S., SATO, K., MIYAJI, T., MATSUMOTO, K., ASAKI, Y., YASUDA, S. and NAKAMURA, S. (1994): in these proceedings.
- VALTAOJA, E., LÄHTEENMÄKI, A. and TERÄSRANTA, H. (1992): *Astron. Astrophys. Suppl. Ser.*, **95**, 73.